Increased efficiency of luminescent solar concentrators after application of organic wavelength selective mirrors

Increased efficiency of luminescent solar concentrators after application of organic wavelength selective mirrors

Paul P. C. Verbunt,[1,] Shufen Tsoi,[1] Michael G. Debije,[1,*] Dirk. J. Broer,[1] Cees W.M. Bastiaansen,[1,2] Chi-Wen Lin,[3] and Dick K. G. de Boer[3]

[1] *Department of Chemical Engineering and Chemistry, Eindhoven University of Technology, P. O. Box 513, Eindhoven, 5600 MB, The Netherlands*

[2]*School of Engineering and Material Science, Queen Mary University of London, London E1 4NS, UK*

[3]*Philips Research Europe, High Tech Campus 4, 5656AE Eindhoven, The Netherlands*

**m.g.debije@tue.nl*

Abstract: Organic wavelength-selective mirrors are used to reduce the loss of emitted photons through the surface of a luminescent solar concentrator (LSC). A theoretical calculation suggests that application of a 400 nm broad reflector on top of an LSC containing BASF Lumogen Red 305 as a luminophore can reflect 91% of all surface emitted photons back into the device. Used in this way, such broad reflectors could increase the edge-emission efficiency of the LSC by up to 66%. Similarly, 175 nm broad reflectors could increase efficiency up to 45%. Measurements demonstrate more limited effectiveness and dependency on the peak absorbance of the LSC. At higher absorbance, the increased number of internal re-absorption events reduces the effectiveness of the reflectors, leading to a maximum increase in LSC efficiency of ~5% for an LSC with a peak absorbance of 1. Reducing re-absorption by reducing dye concentration or the coverage of the luminophore coating results in an increase in LSC efficiency of up to 30% and 27%, respectively.

OCIS codes: (230.1480) Bragg reflectors; (230.3720) Liquid-crystal devices; (230.7408) Wavelength filtering devices; (310.6860) Thin films, optical properties; (350.6050) Solar energy.

References and links

1. W. H. Weber and J. Lambe, "Luminescent greenhouse collector for solar radiation," Appl. Opt. **15**(10), 2299–2300 (1976).
2. A. Goetzberger and W. Greube, "Solar energy conversion with fluorescent collectors," Appl. Phys., A Mater. Sci. Process. **14**, 123–139 (1977).
3. J. A. Levitt and W. H. Weber, "Materials for luminescent greenhouse solar collectors," Appl. Opt. **16**(10), 2684–2689 (1977).
4. G. Seybold and G. Wagenblast, "New perylene and violanthrone dyestuffs for fluorescent collectors," Dyes Pigments **11**(4), 303–317 (1989).
5. R. Reisfeld, D. Shamrakov, and C. Jorgensen, "Photostable solar concentrators based on fluorescent glass films," Sol. Energy Mater. Sol. Cells **33**(4), 417–427 (1994).
6. M. G. Debije, P. P. C. Verbunt, P. J. Nadkarni, S. Velate, K. Bhaumik, S. Nedumbamana, B. C. Rowan, B. S. Richards, and T. L. Hoeks, "Promising fluorescent dye for solar energy conversion based on a perylene perinone," Appl. Opt. **50**(2), 163–169 (2011).
7. A. J. Chatten, K. W. J. Barnham, B. F. Buxton, N. J. Ekins-Daukes, and M. A. Malik, "A new approach to modelling quantum dot concentrators," Sol. Energy Mater. Sol. Cells **75**(3-4), 363–371 (2003).
8. S. J. Gallagher, B. Norton, and P. C. Eames, "Quantum dot solar concentrators: Electrical conversion efficiencies and comparative concentrating factors of fabricated devices," Sol. Energy **81**(6), 813–821 (2007).
9. V. Sholin, J. D. Olson, and S. A. Carter, "Semiconducting polymers and quantum dots in luminescent solar concentrators for solar energy harvesting," J. Appl. Phys. **101**(12), 123114 (2007).
10. G. V. Shcherbatyuk, R. H. Inman, C. Wang, R. Winston, and S. Ghosh, "Viability of using near infrared PbS quantum dots as active materials in luminescent solar concentrators," Appl. Phys. Lett. **96**(19), 191901 (2010).

#167895 - $15.00 USD Received 2 May 2012; revised 12 Jun 2012; accepted 15 Jun 2012; published 18 Jul 2012

11. M. G. Debije and P. P. C. Verbunt, "Thirty years of luminescent solar concentrator research: Solar energy for the built environment," Adv. Energy Mater. **2**(1), 12–35 (2012).
12. M. G. Debije, P. P. C. Verbunt, B. C. Rowan, B. S. Richards, and T. L. Hoeks, "Measured surface loss from luminescent solar concentrator waveguides," Appl. Opt. **47**(36), 6763–6768 (2008).
13. C. W. Oseen, "The theory of liquid crystals," Trans. Faraday Soc. **29**(140), 883 (1933).
14. M. G. Debije, M.-P. Van, P. P. C. Verbunt, M. J. Kastelijn, R. H. L. van der Blom, D. J. Broer, and C. W. M. Bastiaansen, "Effect on the output of a luminescent solar concentrator on application of organic wavelength-selective mirrors," Appl. Opt. **49**(4), 745–751 (2010).
15. D. J. Broer, G. N. Mol, J. A. M. M. V. Haaren, and J. Lub, "Photo-induced diffusion in polymerizing chiral-nematic media," Adv. Mater. (Deerfield Beach Fla.) **11**(7), 573–578 (1999).
16. D. J. Broer, J. Lub, and G. N. Mol, "Wide-band reflective polarizers from cholesteric polymer networks with a pitch gradient," Nature **378**(6556), 467–469 (1995).
17. D. K. G. de Boer, C.-W. Lin, M. P. Giesbers, H. J. Cornelissen, M. G. Debije, P. P. C. Verbunt, and D. J. Broer, "Polarization-independent filters for luminescent solar concentrators," Appl. Phys. Lett. **98**(2), 021111 (2011).
18. D. W. Berreman, "Optics in stratified and anisotropic media: 4x4-matrix formulation," J. Opt. Soc. Am. **62**(4), 502–510 (1972).
19. H. Wöhler, M. Fritsch, G. Haas, and D. A. Mlynski, "Characteristic matrix method for stratified anisotropic media: Optical properties of special configurations," J. Opt. Soc. Am. A **8**(3), 536–540 (1991).
20. N. P. M. Huck, I. Staupe, A. Thirouard, and D. K. G. de Boer, "Light polarization by cholesteric layers," Jpn. J. Appl. Phys. **42**(Part 1, No. 8), 5189–5194 (2003).
21. L. R. Wilson and B. S. Richards, "Measurement method for photoluminescent quantum yields of fluorescent organic dyes in polymethyl methacrylate for luminescent solar concentrators," Appl. Opt. **48**(2), 212–220 (2009).
22. S. Tsoi, D. J. Broer, C. W. Bastiaansen, and M. G. Debije, "Patterned dye structures limit reabsorption in luminescent solar concentrators," Opt. Express **18**(S4 Suppl 4), A536–A543 (2010).
23. S. Tsoi, C. W. M. Bastiaansen, and M. G. Debije, "Enhancing light output of fluorescent waveguides with a microlens system," Proc. 24th Eur. Photovolt. Sol. Energ. Conf., 377–380.
24. O. Moudam, B. C. Rowan, M. Alamiry, P. Richardson, B. S. Richards, A. C. Jones, and N. Robertson, "Europium complexes with high total photoluminescence quantum yields in solution and in PMMA," Chem. Commun. (Camb.) **43**(43), 6649–6651 (2009).
25. K. Barnham, J. L. Marques, J. Hassard, and P. O'Brien, "Quantum-dot concentrator and thermodynamic model for the global redshift," Appl. Phys. Lett. **76**(9), 1197–1199 (2000).
26. D. K. G. de Boer, D. J. Broer, M. G. Debije, W. Keur, A. Meijerink, C. R. Ronda, and P. P. C. Verbunt, "Progress in phosphors and filters for luminescent solar concentrators," Opt. Express **20**(S3), A395–A405 (2012).

1. Introduction

Luminescent solar concentrators (LSCs) were originally introduced as inexpensive replacements for traditional silicon photovoltaic panels in the 1970s [1–3]. LSCs are basically plastic or glass waveguides containing or topped with a thin layer of fluorescent materials, like organic dyes [4–6] or quantum dots [7–10]. These luminophores absorb incident sunlight and re-emit these photons at longer wavelengths. A fraction of emitted photons are trapped inside the waveguide via total internal reflection and transported towards the edge(s). At the edge(s) of the waveguide the photons are collected by small photovoltaic cell(s) (PV(s)) that convert the photons into electrical current. Some potential advantages of LSCs are that they can be made in different colors and shapes, they may be flexible and they can be used in both direct and indirect sunlight. These advantages make LSCs interesting for building integrated energy harvesting [11].

The delay in commercialization of LSCs has been due to a number of loss mechanisms that limit their efficiency. One of the primary losses is a significant fraction of the emitted light escaping the top and bottom surfaces because they are emitted in the escape cone of the waveguide. Measurements have shown that 40-50% of all absorbed energy (50-60% of all absorbed photons) are lost through the surfaces of LSCs containing BASF Lumogen F Red 305 (called Red 305 in the rest of this paper) [12]. Redirection of these surface losses back into the device could lead to an increase in edge emission and overall improvement of the device-efficiency. Wavelength selective mirrors which transmit light that can be absorbed by the luminophore, but reflect photons that are emitted can be used to redirect the surface lost photons back into the LSC. A picture of the working principle is shown in Fig. 1.

#167895 - $15.00 USD Received 2 May 2012; revised 12 Jun 2012; accepted 15 Jun 2012; published 18 Jul 2012

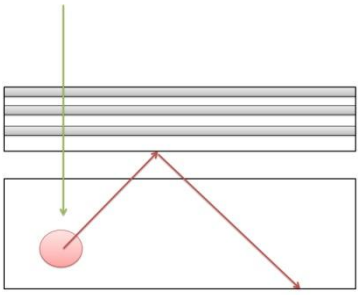

Fig. 1. The working principle of wavelength selective mirrors. Green photons in the solar spectrum are transmitted by the reflector and absorbed by the dye molecules within the waveguide. Red emitted photons are reflected back into the device.

Wavelength selective mirrors can be produced from chiral nematic liquid crystalline (LC) materials (termed 'cholesterics'), which act as Bragg reflectors [13]. Cholesteric materials are nematic liquid crystals where the director of the liquid crystal rotates through the thickness of the film. Due to this rotation, a sinusoidal change of the refractive index is created through the depth of the layer, resulting in reflection if the pitch is on the same length-scale as the wavelength of the light. The wavelength reflected Eq. (1) by the cholesteric is dependent on the pitch of the helix and the refractive index of the host LC. The pitch is the distance it takes the director of the cholesteric material to rotate by 360 degrees.

$$\bar{\lambda} = \bar{n}p \tag{1}$$

where $\bar{\lambda}$ is the center wavelength of the reflection band, $\bar{n}$ is the average refractive index of the LC and p is the pitch.

Previous research has shown that the application of an organic wavelength-selective mirror with a reflection bandwidth of approximately 75 nm led to a reduction in surface loss of up to 35% and an efficiency increase of the LSC up to 12% [14]. The reflection band of the mirrors used in those experiments was not broad enough to reflect all the emitted light from the dye back in the LSC. The reflection band of a cholesteric reflector shifts to shorter wavelengths when the incident angle of the photons becomes larger. This angular dependency can be described by:

$$\overline{\lambda_\theta} = \overline{\lambda_0}\cos\left[\sin^{-1}\left(\frac{\sin\theta}{\bar{n}}\right)\right] \tag{2}$$

where $\overline{\lambda_\theta}$ is the center reflection wavelength at the angle θ, $\overline{\lambda_0}$ is the central reflection wavelength at perpendicular incidence and $\bar{n}$ is the average refractive index of the LC forming the cholesteric phase. Due to the narrow band, the cholesteric layer will not be reflective towards surface emitted photons which encounter the cholesteric reflector at larger angles. It would be an advantage to make selective mirrors with a broader reflection band from solution-cast cholesterics.

The width of the reflection band is determined by two parameters, the pitch and the birefringence of the liquid crystal since,

$$\Delta\lambda = p\Delta n \tag{3}$$

where $\Delta\lambda$ is the width of the reflection band and Δn is the birefringence of the LC [15].

#167895 - $15.00 USD Received 2 May 2012; revised 12 Jun 2012; accepted 15 Jun 2012; published 18 Jul 2012

Broadband organic reflective layers can be made in three ways; (1) by using liquid crystals with a large birefringence, (2) by making a cholesteric layer with a gradient pitch [16,17], and (3) by layering narrowband reflectors with shifted reflection bands.

In this paper we present calculations of the reflection of broadband wavelength selective mirrors made from chiral nematic liquid crystals, and calculate the effect of these reflectors on the performance of LSCs once they are applied on top of the waveguide. Finally, we compare these computational results with experimental measurements.

2. Theoretical approach

The reflective properties of chiral nematic liquid crystalline films can be calculated using Berreman's 4x4 matrix method [18] for light propagation through multilayered homogenous anisotropic media [19]. This method allows calculation of the optical properties of homogenous anisotropic media at oblique incidences. The cholesteric reflector is divided in several homogeneous slabs with a different direction for the optical axis in each slab. This method has been proven to acceptably reproduce the angular dependence of optical transmission and reflection properties experimentally determined for cholesteric reflectors [17,20].

Optical properties of narrowband and broadband cholesteric layers made by three different methods (described above) have been calculated. Reflectors were generated from layering two narrow band reflectors, the ordinary and extraordinary refractive indexes were taken from the commercial liquid crystal host BASF LC242, and the pitches of the separate layers were chosen in such a way so that the overall reflection band was continuous and the broadness of the resulting reflection band was 150-200 nm. For the gradient pitch reflectors, input data was chosen from the materials described by Broer et al. [16] and the pitch gradient was chosen in such a way that the reflection bands were similar to the reflectors made by layering narrow band cholesterics, and the broadness of the reflection band was 400 nm. For the high birefringent material, the characteristics of the liquid crystal BASF LC1057 were chosen. This latter material leads to reflectors with a more narrow reflection band than the two other methods. To match the width of the reflection band of the other two broadband reflectors, unrealistic physical properties would be necessary (i.e. a Δn of 0.4 to create a 175 nm broad reflector with an onset wavelength around 600 nm). Due to the lack of available materials to experimentally produce the desired broadbands in this way, reflectors made from high birefringent materials are not considered in the rest of this paper.

Cholesteric reflectors only reflect one circular polarization of light at perpendicular incidence angle [13]. Right-handed cholesteric reflectors only reflect right-handed circular polarized light and transmit left-circular polarized light. To produce a reflector for unpolarized light, a stack of two cholesterics with opposite handedness is required, or two cholesteric reflectors with the same handedness separated by a half-wave retarder. The simulated reflection properties of the two broadband cholesteric reflectors (stacked right/left and stacked right/right with a halfwave plate between them) for all angles of incidence in air are depicted in Fig. 2.

#167895 - $15.00 USD Received 2 May 2012; revised 12 Jun 2012; accepted 15 Jun 2012; published 18 Jul 2012

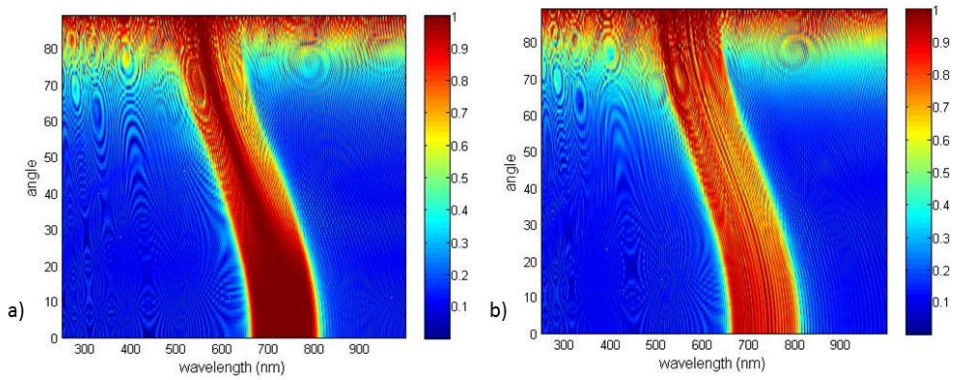

Fig. 2. The simulated reflective properties of 150 nm broad reflectors made from gradient pitch cholesterics. (a) The reflectivity of a full reflector made by stacking a right- and a left-handed cholesteric on top of each other and (b) the reflectivity of a full reflector made by right handed cholesterics on both sides of a half wave retarder centered at 560 nm are used to make a full reflector. The color in these plots represents the reflectivity of the cholesteric reflectors; dark blue is 0% reflection and dark red is 100% reflection.

Figure 2 demonstrates the properties of a reflector made from stacking a right- and a left-handed cholesteric, and shows up to 100% reflection over the entire width of the reflection band when the incidence light is at small angles (up to 20 degrees). When the angle of the incident light becomes larger, the reflective properties begin to decrease starting from the edges of the reflection band. The right picture shows that the reflectivity of two right handed cholesteric reflectors on both sides of a half wave retarder centered at 560 nm is not as constant over the width of the reflection band at small angles of incidence, because the half wave retarder is not completely converting right circular polarized light into left circular polarized light at the wavelengths where the reflector is positioned. When a half-wave retarder is used centered in the same wavelength regime as the reflection band the reflective properties are similar to the properties of a reflector made from stacked right- and left-handed cholesteric reflectors. In the experimental verification we consider stacked narrowband right-handed cholesterics on both sides of a half-wave retarder, in this case centered at 560 nm. For comparison between the theoretical calculations and the experiments we calculated the properties of reflectors made via this method as well as right and left stacked reflectors.

The wavelength selective mirrors are placed on top of an LSC to reflect photons normally escaping through the top surface of the LSC back in the waveguide. Underneath the waveguide a perfect reflector is placed reflecting all photons lost through the bottom of the waveguide. These photons are assumed to not be re-absorbed by the luminophores and subsequently lost again through the top surface. To calculate the increase in LSC efficiency after application of such a reflector, it is necessary to first calculate the reflection efficiency (η_{refl}) of the reflector towards dye-emitted light Eq. (4).

$$\eta_{refl} = \frac{\iint_{photons_{surface}} E_s(\lambda) r(\theta,\lambda) E_p(\theta) d\theta d\lambda}{\iint_{photons_{surface}} E_s(\lambda) E_p(\theta) d\theta d\lambda} \tag{4}$$

where $E_s(\lambda)$ is the emission spectrum of the dye molecules, $r(\theta,\lambda)$ is the reflection spectrum of the reflector as a function of incidence angle of illumination and $E_p(\theta)$ is the angular emission profile of the dye molecules. The efficiency of reflectors with different reflection bandwidths has been calculated for broadband reflectors made from cholesterics

#167895 - $15.00 USD Received 2 May 2012; revised 12 Jun 2012; accepted 15 Jun 2012; published 18 Jul 2012

with a gradient pitch. Two gradient pitch reflectors have been considered, one twice the width of the reflection band of the narrowband reflectors and one with a reflection bandwidth of 400 nm, approximately 5-6 times the width of the reflection band of narrowband reflectors. The efficiency of reflecting surface emitted light is depicted in Fig. 3 for an LSC using Red 305 (see Fig. 4 for the absorption and emission spectra of this luminophore). In these calculations the emission profile of the dyes is assumed to be isotropic. The onset wavelength is defined as the wavelength on the short wavelength side of the reflection band where the reflectivity is 50% of the reflectivity within the reflection band.

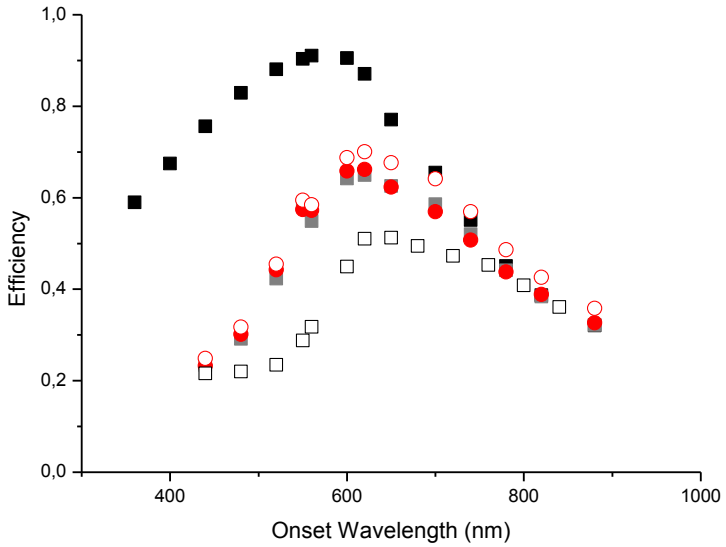

Fig. 3. Calculated efficiency of cholesterics in reflecting light emitted from the top surface of a Red 305 containing LSC for narrowband reflectors (white squares), 175 nm broad gradient pitch reflectors (grey squares), 400 nm broad gradient pitch cholesteric reflectors (black squares), layered reflectors made from 2 narrowbands (filled red circles for stacked right and left handed reflectors and open red circles for stacked right handed reflectors on both sides of a half wave retarder centered at 560 nm) as a function of the onset wavelength of the cholesteric reflectors.

The efficiency of all the cholesteric reflectors is equal at longer onset wavelengths and increases for shorter wavelengths. The efficiency peaks when the cholesteric onset wavelength is in the spectral part of the emission by the luminophore. The efficiency of reflector with the broadest reflection band (~400 nm) peaks at the shortest wavelength. All reflectors exhibit a blue shift for high angles, but for the broad cholesteric reflector the complete emission band of the luminophore is in the reflection band at all angles, so the highest efficiency is reached if the onset wavelength of the reflector is close to the onset wavelength of the emission band. The reflectors with the smaller reflection bands are not broad enough to reflect all the emitted light over all angles emerging from the surface, and so the efficiency of these reflectors peaks at slightly longer wavelengths. The maximum efficiencies with corresponding onset wavelengths are shown in Table 1.

#167895 - $15.00 USD Received 2 May 2012; revised 12 Jun 2012; accepted 15 Jun 2012; published 18 Jul 2012

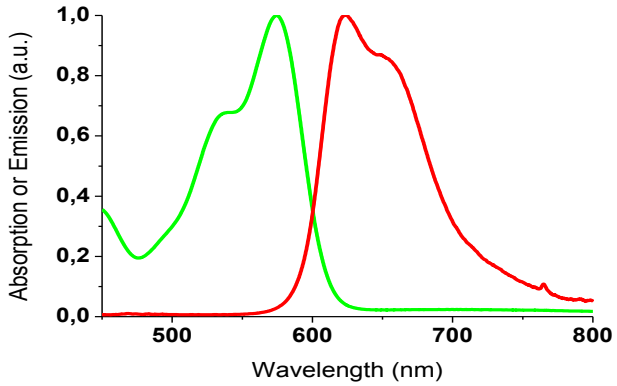

Fig. 4. Normalized absorption and emission spectrum of Red 305 in polycarbonate.

Table 1. Maximum Reflection Efficiency of the Cholesteric for Surface Emitted Light of LSCs Containing Red 305 as Luminophore

Reflector	Maximum efficiency	Onset Wavelength (nm)
400 nm gradient pitch	91%	560
175 nm gradient pitch	65%	620
75 nm narrowband	51%	650

The 175 nm broad reflectors made from gradient pitch cholesterics and from layered narrowband reflectors show similar efficiencies at all onset wavelengths. This shows that the broadness of the reflection band is more important for the efficiency than the method by which the reflectors are made.

However, cholesteric reflectors may also reflect incoming sunlight away from the device, resulting in reduced absorption if the reflection band coincides with the absorption spectrum of the dye. This feature must also be included in a calculation as to how effective the cholesteric reflectors could prove on top of an LSC. The fraction of light that is absorbed by the luminophore that passes through the cholesteric filter (f_{chol}^{EA}) can be described by

$$f_{chol}^{EA} = \frac{\int I(\lambda) * (1 - r(\lambda)) * A(\lambda) d\lambda}{\int I(\lambda) * A(\lambda) d\lambda} \tag{5}$$

where $I(\lambda)$ is the intensity of the incident light (in this case, the solar spectrum), $A(\lambda)$ is the absorption spectrum of the dye and $r(\lambda)$ is the reflection spectrum of the cholesteric filter at perpendicular incidence. In this calculation it is assumed that only direct sunlight is incident normal to the LSC device. The results are depicted in Fig. 5.

When the onset reflection wavelength is outside the absorption range of the luminophore, the reflectors transmit approximately 90% of all the absorbable light; the 10% loss results from the fact the cholesteric reflector is added to the LSC with an airgap creating two additional surfaces and extra Fresnel reflections. As the onset wavelength of the cholesteric reflectors passes into the absorption range of the luminophores, the amount of absorbable incident light that is transmitted through the reflector decreases drastically. This decrease is approximately equal for all reflectors and is thus not influenced by reflection band broadness or production method.

#167895 - $15.00 USD Received 2 May 2012; revised 12 Jun 2012; accepted 15 Jun 2012; published 18 Jul 2012

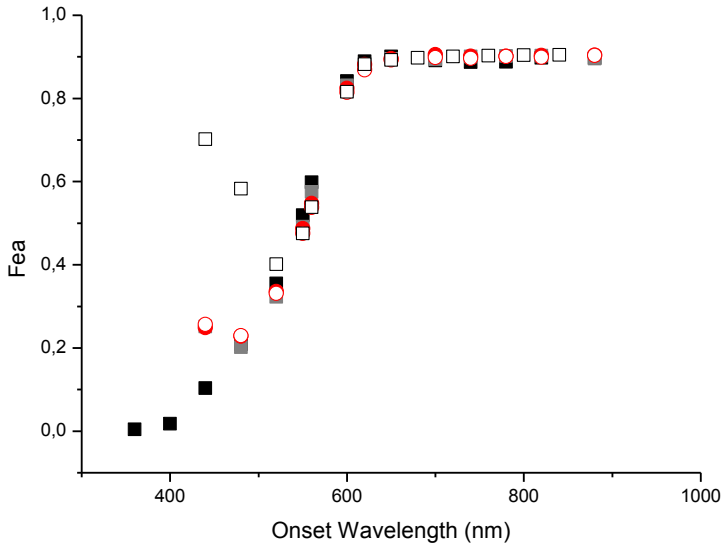

Fig. 5. The fraction of the incoming sunlight within the absorption band of the dye that could be absorbed by the luminophore (Red 305) that passes through the cholesterics (F_{ea}) made from narrowband reflectors (white squares), 175 nm broad gradient pitch reflectors (grey squares), 400 nm broad gradient pitch cholesteric reflectors (black squares), layered reflectors made from 2 narrow bands (filled red circles for stacked right and left handed reflectors and open red circles for stacked right handed reflectors on both sides of a half wave retarder centered at 560 nm).

The maximum total increase in LSC efficiency ($\eta_{LSC,\max}$) is a combination of both incident and emitted light reflection and can be calculated from the efficiency of the reflector and the absorbable incident light that passes through the reflector. This increase can be described by the number of photons leaving the edge of the LSC when a cholesteric filter is added ($n_{edge,chol}$) and the number of photons leaving the edge of the LSC without a cholesteric filter ($n_{edge,bare}$).

$$\eta_{LSC,\max} = \frac{n_{edge,chol}}{n_{edge,bare}} = \frac{f_{chol}^{EA} n_{edge,bare}}{n_{edge,bare}} + \frac{n_{edge,SL,chol}}{n_{edge,bare}} \tag{6}$$

where $n_{edge,SL,chol}$ is the total number of photons formerly lost through the surface that are converted to edge emission of the LSC due to addition of the cholesteric and defined as:

$$n_{edge,SL,chol} = f_{chol}^{EA} * QE * \phi_{SL} * \eta_{chol} \tag{7}$$

and

$$n_{edge,bare} = QE * \phi_{wm} \tag{8}$$

where QE is the fluorescence quantum yield of the luminophore, and ϕ_{wm} and ϕ_{SL} are the fractions of emitted photons in waveguide mode and surface loss mode (i.e. within the escape cone) respectively.

#167895 - $15.00 USD Received 2 May 2012; revised 12 Jun 2012; accepted 15 Jun 2012; published 18 Jul 2012

Although a complete calculation of $\eta_{LSC,\max}$ requires a detailed knowledge of the processes in the waveguide, a rough estimate can be obtained in the following way; for a waveguide containing Red 305 it was previously shown [12] that the number of photons in surface loss mode was approximately 50% of all absorbed photons for 5x5 cm^2 LSCs made from polycarbonate and a peak absorption above 0.3. Since the fluorescence quantum yield of Red 305 is nearly unity [21] the part of the emitted photons in waveguide mode is also approximately 50%, so ϕ_{wm} and ϕ_{SL} can be assumed equal leading to

$$\eta_{LSC,\max} = f_{chol}^{EA}\left(1+\eta_{chol}\right) \tag{9}$$

In this calculation, all the light reflected back in the LSC by the cholesteric reflector is assumed to reach the edge of the LSC. Thus, there is only one interaction with the reflector and there is no re-absorption of these back-reflected photons, losses from parasitic waveguide absorption, or other such events. The results are depicted in Fig. 6.

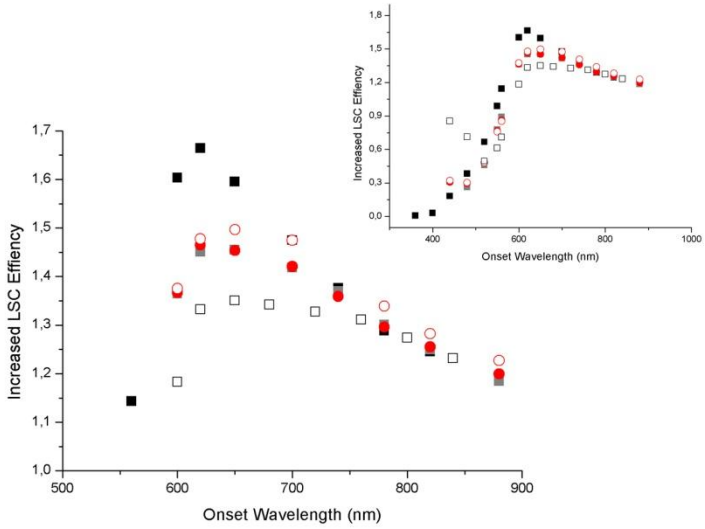

Fig. 6. The calculated maximum possible increase in LSC efficiency after application of cholesteric reflectors to an LSC containing Red 305 as a luminophore. The reflectors are made from narrowband cholesterics (white squares), 175 nm broad (grey squares) and 400 nm broad gradient pitch cholesteric (black squares), layered cholesteric and reflectors made from 2 narrowbands (red circles for stacked right and left handed reflectors and open red circles for stacked right handed reflectors on both sides of a half wave retarder centered at 560 nm). The main graph is an enlargement of the graph region which gave an increase in efficiency; the inset shows all data.

With the broadening of the reflection band, the maximum possible increase in LSC efficiency improves. The onset wavelength of the cholesteric where the efficiency increase is the highest is red-shifted with respect to the emission peak of the luminophore, but for the broadest reflector the red-shift is less pronounced than for the narrower reflectors. The maximum possible increase in LSC efficiency and the corresponding onset wavelength of the cholesteric are shown in Table 2.

By adding a 400 nm broad reflector at the top of an LSC, the efficiency could be increased by up to 66%. If a reflector with a more narrow reflection band is added to the top of the LSC, increases of 45% or 35% could be achieved for 175 nm broad reflectors and 75 nm broad reflectors, respectively.

#167895 - $15.00 USD Received 2 May 2012; revised 12 Jun 2012; accepted 15 Jun 2012; published 18 Jul 2012

Table 2. Maximum Calculated Increase in LSC Efficiency after Addition of the Cholesteric Reflectors to LSCs Containing Red 305 as Luminophore

Reflector	$\eta_{LSC,\max}$	Onset wavelength (nm)
400 nm gradient pitch	1.66	620
175 nm gradient pitch	1.45	650
75 nm narrowband	1.35	650

As described in the next Section, 175 nm broad cholesteric reflectors were made from right-handed layered narrowband reflectors on either side of a half wave retarder centered at 560 nm and placed on top of Red 305 LSCs. The results of these measurements and a comparison with the theoretical results described in this paragraph are shown and discussed in section 4.

3. Experimental

The broadband reflectors were made from two stacked right-handed narrowband reflectors applied to a manually rubbed half wave plate centered at 560 nm (Edmund Optics). A mixture of reactive LC mesogen LC242 (BASF), varying concentrations chiral dopant LC756 (BASF), 1% of photoinitiator Irgacure 184 (Ciba) and 1% of surfactant to induce planar alignment at the liquid crystal-air interface in xylene (1:1 by weight, Aldrich) were spin coated at 800 rpm for 30 seconds. After spincoating, the samples were immediately heated on a hot stage at 90 °C for 30 seconds and then photo-polymerised by UV-exposure in a nitrogen atmosphere. Before applying the second reflecting layer with a higher concentration of chiral dopant, the first layer was treated with an oxygen-plasma for 1 minute at 60W, to improve the wetting of the LC layer. A similar process was applied to the rear side of the same halfwave plate following an identical procedure.

The filled waveguides were produced by injection molding (poly)carbonate doped with 5-180 ppm BASF Lumogen F Red 305 into 50 x 50 x 3 mm^3 plates (Sabic IP). The patterned LSC waveguides were produced on PMMA plates (50 x 50 x 5 mm^3) (Plano Plastics). Fluorescent dye solutions were prepared using 0.5% wt of Red 305, and 1% photoinitiator (Irgacure 184) dissolved in a 3:1 dipentaerythritol penta-acrylate (Polysciences) and methylmethacrylate (MMA, Aldrich) blend. The dye solutions were stirred and heated at 60°C for an hour prior to spin-coating onto the substrates at 1000 rpm for 30 s. After spin-coating, all 100% covered samples were crosslinked by exposing to a high-intensity UV lamp for 80 s under nitrogen flow to form a solid film. For the fabrication of patterned LSCs (see Section 4 of this paper), standard photolithography techniques were employed. Uniformly coated substrates were exposed to UV light through patterned shadow masks consisting of 10 lines with variable widths with a period of 5 mm. Line widths were varied to cover 20 to 80% of the waveguide surface. After UV exposure, ethanol was used to etch away the unexposed material on the PMMA substrates. The exposed patterned samples were placed in ethanol for 40 s at room temperature and the samples were continuously agitated during the etching process.

Transmission spectra of the manufactured reflectors and absorption spectra of the waveguides were recorded with a Shimadzu UV-3102 spectrophotometer. The edge emissions from the LSC waveguides with and without broadband reflectors were recorded using an SLMS 1050 integrating sphere equipped with a diode array detector. The samples were placed with their edges in the entry port of the integrating sphere while illuminated with a 300W solar simulator with filters to approximate the 1.5 AM solar spectrum (Lot Oriel). The spectrum and intensity of the edge emission were recorded. A thick piece of paper (5x5 cm^2) spray painted white was placed underneath the samples to act as a Lambertian scatterer. A schematic depiction of the measurement setup is shown in Fig. 7. The edge emission from all four edges were measured and the total output was determined by integrating the recorded spectra from 350 to 750nm [14].

#167895 - $15.00 USD Received 2 May 2012; revised 12 Jun 2012; accepted 15 Jun 2012; published 18 Jul 2012

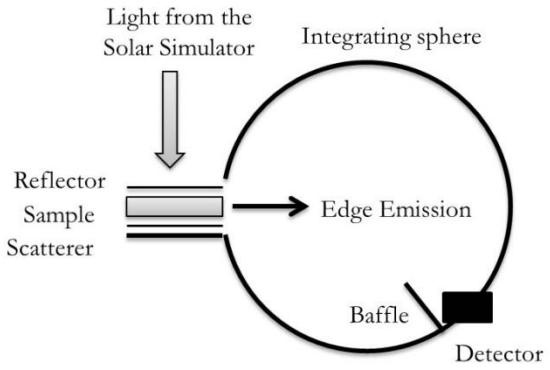

Fig. 7. Schematic depiction of the measurement setup.

4. Results and discussion

Seven broadband reflectors were produced with different onset wavelengths: 620 nm, 660 nm, 700 nm, 740 nm, 780 nm, 820 nm and 880 nm. The reflection bands of these cholesterics were measured and compared to the calculated reflection bands at perpendicular incidence. The differences between the theoretical and experimental spectra are approximately similar for all the different reflectors. As an example, the calculated and experimental spectra of the reflector with an onset wavelength of 740nm are depicted in Fig. 8.

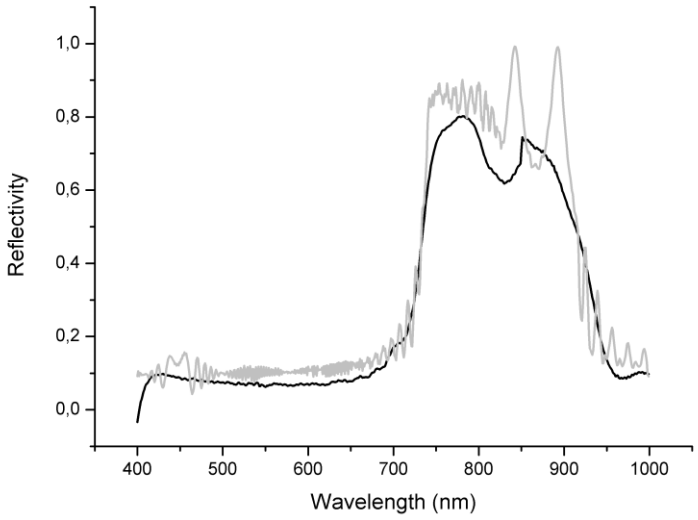

Fig. 8. Reflection spectra of a broadband reflector with an onset wavelength of 730 nm made from 2 layered right handed narrowband reflectors on both sides of a half wave retarder centered at 560 nm, both experimental (black) and calculated (gray).

The experimental spectrum shows that the width of the reflection band is the same as calculated, but the reflectivity is somewhat lower. This reduction can be a result of reduced layer thickness in the manufactured reflector than assumed in the theoretical calculations. Furthermore, the first layer applied experimentally is treated with a plasma asher, which can further reduce the layer thickness. Therefore, reflectivity on the longer wavelength side of the reflection band is slightly lower than on the short wavelength side, since the layer with the

#167895 - $15.00 USD Received 2 May 2012; revised 12 Jun 2012; accepted 15 Jun 2012; published 18 Jul 2012

reflection band at the longer wavelength side of the reflection band was applied first in all cases. The theoretical spectrum demonstrates less than 100% reflectivity caused by the use of the slightly mismatched half wave retarders which do not completely convert left circularly polarized light passing through the right handed cholesterics into right circularly polarized light, so the right handed cholesterics on the back side will not be capable of reflecting all remaining transmitted light.

The cholesteric reflectors were placed on top of (poly)carbonate LSCs filled with Red 305, and the edge emission spectra and intensity (in Watts) measured using an integrating sphere under illumination with a solar simulator (AM 1.5). Underneath the samples, a white Lambertian scatterer was placed. These measurements were compared with the edge output of the same LSC with the white scatterer but without the cholesteric reflector. The ratio between the two edge output intensities is plotted in Fig. 9.

Application of cholesteric reflectors to an LSC with a peak absorbance of approximately 1.0 increased edge output by a maximum of 4.5% when the reflector with the onset wavelength of 700 nm is added: similar increases are seen in samples with higher absorbance (2.36). At lower peak absorption (<0.1) the increase in efficiency is much higher, with a peak increase in efficiency of 30% at 740 nm. However, this is lower than was calculated, and the onset wavelength of the reflector with the maximum increase is red shifted in comparison to the calculations.

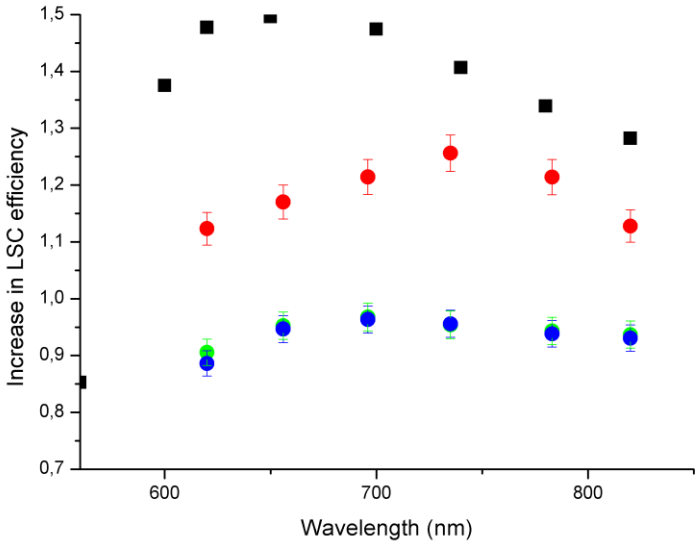

Fig. 9. Relative LSC efficiency after application of broadband reflectors with respect to the LSC without the broadband reflector. The LSCs contain Red 305 with different peak absorbance: calculated (black), 0.05 (red), 1.01 (green), 2.36 (blue).

There are several differences between the theoretical approach and the experimental measurements. First, the reflectivity of the experimental reflectors is not as good as calculated in theory. Second, the theoretical approach assumed that all light reflected back into the LSC by the reflectors reaches the edge of the LSC. In the experiments this is not the case. Photons reflected back into the LSC can be re-absorbed by the luminophores in the LSC due to the overlap in absorption and emission spectra. Reflected photons not immediately absorbed will not be in waveguide mode, so they will encounter the white scatterer underneath the sample, potentially multiple times. If the reflectors have non-unity reflectivity it can result in

#167895 - $15.00 USD Received 2 May 2012; revised 12 Jun 2012; accepted 15 Jun 2012; published 18 Jul 2012

additional losses. Finally, the emission profile is assumed to be spherical for the calculations. In actual practice, the emission profile will not be spherical due to dichroic absorption and emission of the luminophore in combination with the collimated incident light [12]. However, calculations using a non-spherical emission profiles show only small differences with the calculations using spherical emission profiles. The LSC with the very low peak absorbance shows a higher increase in efficiency after application of the cholesteric reflectors, suggesting re-absorption is the primary reason behind the lower experimental increase than predicted.

Tsoi et al. [22,23] demonstrated that patterning the luminophore on a clear waveguide can reduce the amount of re-absorption events. To investigate the influence of re-absorptions on our previous measurements, we determined the impact of adding cholesteric reflectors to patterned LSCs. Waveguides with a pattern of 10 uniformly distributed lines were used, where the widths of the lines determined the coverage of the dye coating on the LSC. The results of these measurements are shown in Fig. 10 using a dye coating with a relatively high peak absorbance (approximately 1) within the patterned areas.

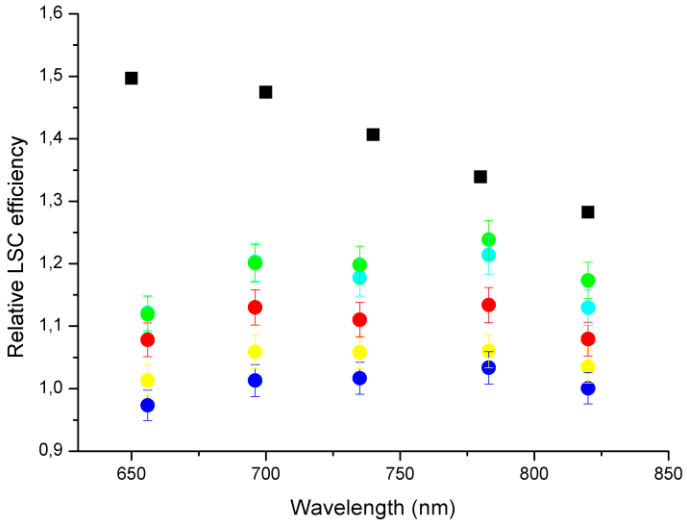

Fig. 10. Relative efficiency of patterned LSCs after application of broadband reflectors with respect to the patterned LSC without the broadband reflector. The LSCs are topped with a coating containing Red 305 with a peak absorbance of 1.0 with different pattern coverage of the surface: calculated (black), 20% (green), 30% (cyan), 50% (red), 70% (yellow), 100% (blue).

The sample with surface coverage of 100% shows the same results as a filled waveguide with approximately the same peak absorbance when topped by a broadband reflector, an increase in efficiency of 5%. Reducing the surface coverage of the coating containing the luminophore, and thus the amount of re-absorption events for emitted light, enhanced the impact of the cholesteric reflectors on the LSC efficiency. The lower the coverage, the higher the increase in efficiency achieved by applying the cholesteric reflectors for all reflectors sampled. The LSC with coverage of 20% shows an increase in edge emission efficiency of up to 27%, although this is still lower than calculated. Furthermore, it can be seen that the application of reflectors with a longer onset wavelength results in an increase in LSC efficiency approaching the theoretical increase better than with a shorter onset wavelength reflectors. This could also be explained if re-absorption is the main cause of the reduced effectiveness of cholesteric reflectors on the experimental increase of LSC-efficiency.

#167895 - $15.00 USD Received 2 May 2012; revised 12 Jun 2012; accepted 15 Jun 2012; published 18 Jul 2012

Re-absorption occurs mostly in the short wavelength part of the emission spectrum of the dye, since the absorption in this region is the highest. Cholesteric reflectors with an onset wavelength close to the onset wavelength of the emission of the dye will reflect this emitted light for most of the angles of incidence. The reflectors with a longer onset wavelength will only reflect these photons that have a larger probability for being re-absorbed at larger angles. Thus, the effect of re-absorption in LSCs using short onset wavelength reflectors is larger than for longer onset wavelength reflectors. These results demonstrate that re-absorption has a large influence on the effectiveness of the reflectors. Since the experimental increase in the LSC with a low amount of re-absorption after application of the cholesteric reflectors is still lower than calculated for all applied reflectors, it can be assumed that the multiple interactions of the back reflected photons with the reflectors also have an influence on the effectiveness of the cholesteric. The experimental reflectors were not ideal (reflectivity was < 100% within the reflection bandwidth), so there was the possibility of a small loss of light at each encounter. The quality of the reflectors will become even more important with increased device size, since the number of interactions of the light with the reflector will also increase if the waveguide thickness is not changed.

5. Conclusion

400 nm broad reflectors made from polymeric cholesteric liquid crystalline films can theoretically reflect over 90% of all surface emitted photons back into an LSC containing Red 305 as a luminophore. However, these cholesterics reflect away a part of the absorbable incident light if the spectral position of the reflector is matched to this maximum efficiency. In theory, the 400 nm broad reflector could increase LSC edge emission efficiency up to 66%. Reflectors with a more narrow reflection band have less impact on the LSC efficiency: 175 nm broad reflectors could increase this efficiency up to 45%. Experiments demonstrate that applying a 175 nm broad reflector to an LSC with Red 305 as a luminophore and a peak absorbance of 1 increases the efficiency of the actual LSC by 5%. The main reason for this discrepancy is the re-absorption of the back reflected photons. When the re-absorption is decreased by lower the peak absorption to a value below 0.1, the increase in LSC efficiency becomes nearly 30%, while lowering the re-absorption by reducing the coverage of dye coating the increase in LSC efficiency reaches 27%. This shows that by reducing the re-absorption of back reflected photons the effectiveness of the cholesteric reflectors increases.

More reproducible, higher-quality reflectors coupled with a reduction in the amount of re-absorptions could make the cholesteric reflectors very effective in enhancing LSC performance. Reducing the number of re-absorptions, while simultaneously maintaining a high absorption of incident light could be achieved by placing lenses on top of the patterned waveguides [23] or by using luminophores with little or no overlap between the absorption and emission bands, such as complexes of rare-earth ions with organic ligands [24], quantum dots [25] or phosphors [26].

Acknowledgments

M.G. Debije acknowledges the support of the Stichting voor Technische Wetenschappen (STW) VIDI grant 7940. The authors would like to thank Sabrina van Oerle, Stéphanie Bex, Matheus Timmers, and Yoran Zonneveld for showing that layering cholesterics is an easy process to make broadband cholesteric reflectors and Merijn Giesbers for adjusting the software, and T. Hoeks of Sabic IP (Bergen op Zoom, the Netherlands) for providing the dye filled polycarbonate plates used in this paper.